A ZEOLITE-COATED BED FOR AIR CONDITIONING ADSORPTION SYSTEMS: PARAMETRIC STUDY OF HEAT AND MASS TRANSFER BY DYNAMIC SIMULATION

G. Restuccia, A. Freni and G. Maggio

CNR - Institute for Transformation and Storage of Energy, S. Lucia sopra Contesse 5, 98126 Messina, Italy.

ABSTRACT

In this paper the heat and mass transfer properties of a new zeolite-coated adsorbent bed to be employed in sorption air conditioning systems are investigated by a modelling approach. It consists of a dynamic model which allows to calculate the exchanged energies, the cycle time and, thus, the specific power of the bed. The analysis of the model results, has shown that the proposed configuration (in which the heat transfer enhancement is mainly related to the good adhesion between metal and adsorbent) is very interesting if compared with the traditional beds. Furthermore, to determine the conditions which allow to obtain the most effective heat and mass transfer in the new adsorbent bed, an optimisation study has been carried out.

KEYWORDS

Adsorption heat pump, adsorbent bed, mass transfer, heat transfer, factorial design.

1. INTRODUCTION

The research activities on closed loop adsorption cycles for air conditioning applications increased very much during last years. In fact, the adsorption machines are considered as an interesting alternative to the vapour compression systems that use highly ozone depleting refrigerants (CFCs or HCFCs). The basic cycle consists of four main components: an adsorber, a condenser, an evaporator and an expansion valve. The adsorber is the "engine" of the machine; it is composed of the adsorbent material (e.g. zeolite) and a heat exchanger for its heating/cooling. A detailed description of the adsorption air conditioning device and its principle of operation is given in literature [1, 2].

The first prototypes for adsorption heating and cooling applications [3, 4] were realised with solid adsorbent bed in non-consolidated forms (zeolite in grains or powder). From the experimental activity on this type of machine, many limits of the system were evidenced; the most important was the low heat transfer and consequently the long duration of the cycle. In fact, the global heat transfer coefficient of the adsorber was very low because of the low thermal conductivity of the porous material employed and also because of the poor thermal contact among the adsorbent grains and between the particles and the surface of heat exchanger. For the above mentioned reasons, the research activity has been addressed to the improvement of heat transfer by both the modification of morphological and thermophysical characteristics of the solid adsorbent and the design of the solid adsorbent/heat exchanger assembly. To this aim, consolidated thick beds with high thermal conductivity were proposed by other research groups [5-7]. However, for those beds, the poor mass transfer of the vapour became a new limiting factor.

A further consolidated bed was proposed by Pino et al. [8], it consisted of zeolite powder with binder pressed by a mould to obtain a brick shape with small thickness.

The planar geometry allowed to obtain a good thermal contact with the surface of the heat exchanger.

In this paper, a different original solution developed at CNR-ITAE is presented; it consists of an adsorbent coating (zeolite-based) firmly bound to the metal of the heat exchanger. The preparation process involves several steps. Initially, an aqueous solution of zeolite powder and an inorganic binder (alumina gel precipitated in-situ) are homogenised. Afterwards, the slurry is layered on the metal support, properly pretreated, in order to obtain a homogenous coating of the desired thickness. A final thermal treatment in air allows the stabilisation of the adsorbent. The technique of coating developed can be applied to different types of heat exchangers (e.g. tube and shell).

This configuration of the adsorbent bed allows to obtain a slight increase of the thermal conductivity of the adsorbent and a strong rise of the metal/adsorbent wall heat transfer coefficient. This result improves the global heat transfer coefficient and, consequently, the specific power of the system. Furthermore, the sufficiently high permeability measured and a small thickness of the adsorbent bed allow to limit the mass transfer resistance.



Figure 1. Photo of the metal-bound zeolite layer.

Figure 1 shows a sample realised following the procedure above described. In this case, a stainless steel tube (type AISI 304, internal diameter 14 mm, thickness 0.4 mm) is coated with 4 mm of adsorbent.

2. MODELING

In this paragraph, the mathematical model realised for the dynamic simulation of a basic cycle of an adsorption device is described. The model considers the heat and mass transfer resistances inside a non-uniform pressure and temperature cylindrical adsorber, neglecting the axial gradients.

A portion of the adsorber is schematised in Figure 2, the components considered are: the heating/cooling fluid (silicon oil), the metal tube of the heat exchanger and the adsorbent bed.

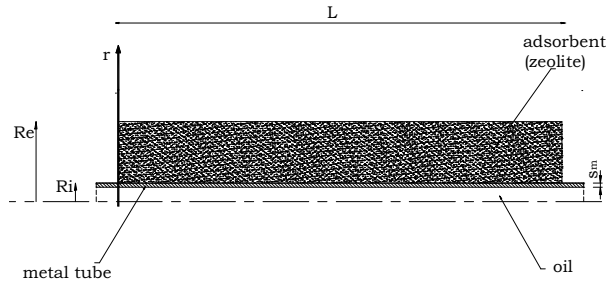


Figure 2. Scheme of the adsorber.

A specific feature of the model is: the equivalent thermal conductivity of the bed λ_{eq} , the equivalent specific heat c_{peq} and the sorption enthalpy ΔH are experimentally obtained as a function of pressure and temperature [9].

The equations that describe the system are the following:

$$\frac{\partial T_{m}}{\partial t} + \frac{h_{fm} A_{fm} (T_{m} - T_{f})}{\rho_{m} c_{pm} V_{m}} + \frac{h_{w} A_{w} (T_{m} - T_{s|m})}{\rho_{m} c_{pm} V_{m}} = 0$$

b) mass balance for the adsorbent bed

$$\varepsilon_{t} \frac{\partial \rho_{v}}{\partial t} + \frac{1}{r} \frac{\partial (r \rho_{v} v_{0})}{\partial r} + (1 - \varepsilon_{t}) \rho \frac{\partial w}{\partial t} = 0$$

c) energy balance for the adsorbent bed

$$(1 - \varepsilon_{t}) \frac{\partial}{\partial t} \left[\rho \left(1 + w \right) c_{peq} T_{s} \right] + \frac{1}{r} \frac{\partial}{\partial r} \left(r \rho_{v} c_{pv} T_{s} v_{0} \right) +$$

$$+ \varepsilon_{t} \frac{\partial \left(\rho_{v} c_{pv} T_{s} \right)}{\partial t} = \frac{\lambda_{eq}}{r} \frac{\partial}{\partial r} \left(r \frac{\partial T_{s}}{\partial r} \right) + (1 - \varepsilon_{t}) \rho \left| \Delta H \right| \frac{\partial w}{\partial t}$$

where $T_{s|m}$ is the temperature of the adsorbent at the adsorbent/metal interface; v_0 is the vapour diffusive velocity, which is determined by Darcy's law $v_0 = -K/\mu_v \cdot \partial p/\partial r$, where the permeability K can be calculated [10, 11], or experimentally determined.

The temperature of the heating/cooling fluid is considered constant ($T_f = T_{oil,h}$ in heating and $T_f = T_{oil,c}$ in

cooling) and the initial and boundary conditions are the

$$T_{m}\Big|_{t=0} = T_{s}\Big|_{t=0} = T_{0}, \qquad p\Big|_{t=0} = p_{0},$$

$$\frac{\partial T_{s}}{\partial r}\Big|_{r=R_{e}} = 0, \qquad -\lambda_{eq} \frac{\partial T_{s}}{\partial r}\Big|_{r=R_{i}} = h_{w} (T_{m} - T_{s}),$$

$$p\Big|_{r=R_{e}} = p_{ev/con} \qquad \text{ad/desorption phase,}$$

$$\frac{\partial p}{\partial r}\Big|_{r=R_o} = 0$$
 isosteric heating/cooling phase,

where $p_{ev/con}$ is the pressure of the evaporator/condenser. The differential equations were solved with an implicit finite difference method (Crank-Nicholson [12]). The model calculates the pressure, temperature and water uptake distribution in the bed as a function of time. Furthermore, the coefficient of performance of the adsorption machine working as heat pump and refrigerator are calculated as:

$$COP_h = \frac{Q_c + Q_{con}}{Q_h}, \quad COP_c = \frac{Q_{ev}}{Q_h},$$

where Q_h is the heat supplied for the desorption of the adsorbent bed, Q_c is the heat released from the bed during the cooling, Q_{con} is the heat released to the condenser and Q_{ev} is the heat extracted from the evaporator.

The corresponding specific powers are defined as:

$$Ps_h = \frac{Q_c + Q_{con}}{m_s t_{cycle}}, \quad Ps_c = \frac{Q_{ev}}{m_s t_{cycle}},$$

where t_{cycle} is the total cycle time.

3. SIMULATION RESULTS

Simulations have been performed by using the geometrical and thermo-physical input data reported in Tables 1-2. The operating conditions are typical of an air conditioning cycle.

The model was initially used to compare four types of adsorbent bed that, as above mentioned, differ in terms of shape of the adsorbent (Table 2): grains [13], powder [13], brick [14], and the coating layer here proposed.

Results presented in Figure 3 show that the specific power obtained with the new bed configuration is the best (600 W kg⁻¹), and about twenty times higher than that of the bed in grains.

A surprising result is that the power obtained with the brick-shaped bed is lower than that of the nonconsolidated powder. This can be related to the fact that the increased heat transfer properties of the brickshaped bed is not sufficient to increase the specific power of the machine because of the low adsorbate diffusivity within the adsorbent layer. These results show the interrelated influence of the heat and mass transfer properties of the bed on the performance of the air conditioning systems. The parameters affecting the heat transfer in the bed are the equivalent thermal conductivity λ_{eq} , and the metal/adsorbent heat transfer

coefficient h_w . The mass transfer of the adsorbate within the adsorbent can be considered by means of the adsorbent permeability to the vapour K. Finally, the adsorbent thickness s is a parameter affecting both the heat and mass transfer.

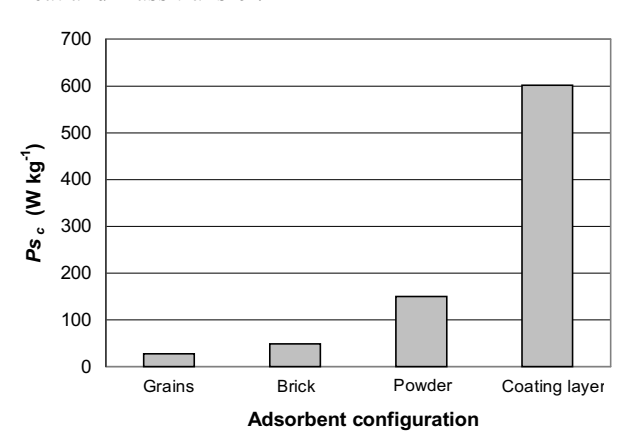


Figure 3. Comparison of calculated specific power of different adsorbent configurations.

In order to study the mutual influence of the above mentioned parameters, a full factorial design method was applied to the new bed configuration developed at CNR-ITAE.

Once defined the normalised variables:

$$x_i^* = \frac{x_i - (x_i^+ + x_i^-)/2}{(x_i^+ - x_i^-)/2},$$

where x_i^- e x_i^+ are the lower and upper limits of the x_i variables, according to the formalism of the full factorial design method, a studied function is defined as follows:

$$y = m_0 + \sum_{i} m_i x_i^* + \sum_{j} \sum_{i < j} m_{ij} x_i^* x_i^* + \dots + m_{123...n} x_i^* x_i^* \dots x_n^*$$

where m_0 describes the mean effect of all the n parameters, $m_1, \ldots m_n$ the effect of each parameter and $m_{ij}, m_{ijk} \ldots$ etc. the effect of the interaction of the parameters. Further details are reported in literature [15, 16].

In our case, the studied function is the specific cooling power and the analysed parameters are: the adsorbent/metal wall heat transfer coefficient, the vapour permeability, the thickness and the equivalent thermal conductivity of the adsorbent bed. The lower and upper limits of these parameters are reported in Table 3.

The results of this study show that the parameters that have the strongest influence on the specific power are the thickness of the bed and the permeability. This is shown in Table 4 and Figure 4, where the calculated mean effect of each parameter on the specific power is reported. The values reported represent the mean

variation of the specific power due to the change, from the lower to the upper limit, of each of the four parameters.

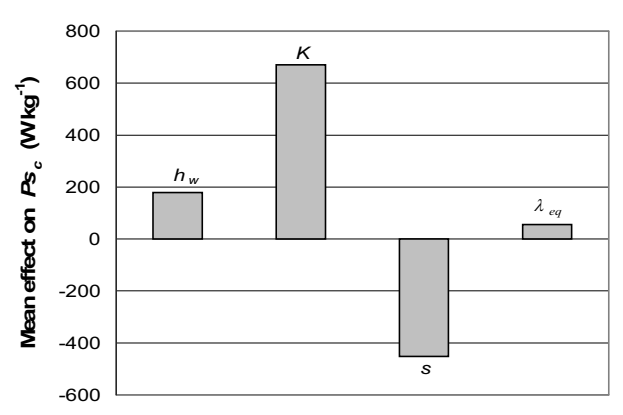


Figure 4. Full factorial design: mean effect of the selected parameters on the studied function.

By analysing the results of the simulations performed for the bed realised with the coating technique, it is possible to put in evidence (Figure 5) the strong influence of the permeability on the specific cooling power of the machine.

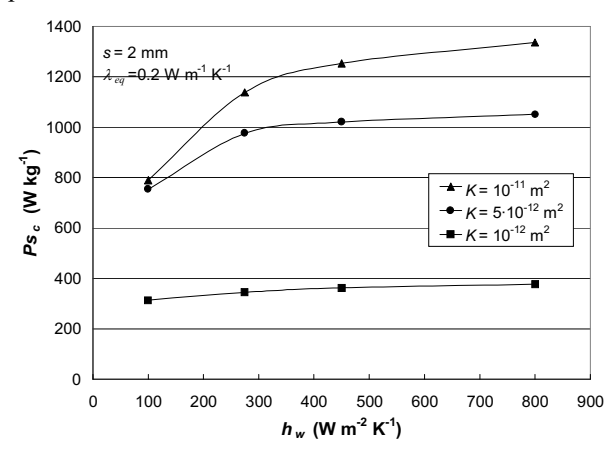


Figure 5. Influence of the wall heat transfer coefficient on calculated specific power, for s^- and λ_{eq}^- (see Tab. 3).

This effect is evidenced for $h_w > 300\text{-}400 \text{ W m}^{-2} \text{ K}^{-1}$ that are surely obtained with the coating technique. On the contrary, for low values of the wall heat transfer coefficient the influence of the mass transfer resistance decreases. Furthermore, Figure 5 shows that, even if the thermal conductivity is low (λ_{eq} =0.2 W m⁻¹ K⁻¹), with the new bed proposed it is possible to obtain a very high specific cooling power, providing that the bed thickness is low and the permeability is higher than K=5·10⁻¹² m².

Figure 6 shows that by increasing the adsorbent thickness the specific power drastically decreases even if the thermal conductivity increases.

The effect of the equivalent thermal conductivity of the bed, is shown in Figure 7. It affects the specific cooling power for permeability $K=10^{-11}$ m² or higher.

Finally, Figure 8 puts in evidence the strong influence of the bed thickness *s* on the specific power; this result is not surprising because *s* influences both the mass and heat transfer.

The analysis of the Figures 5-8 shows that, for consolidated bed, is useless to increase the heat transfer parameters if the adsorbent thickness is low and the vapour permeability is not sufficiently high.

Furthermore, it was shown that high values of Ps_c can be obtained with low values of λ_{eq} if the mass transfer and the thermal contact metal/adsorbent are efficient. This consideration agrees with our strategy of bed design.

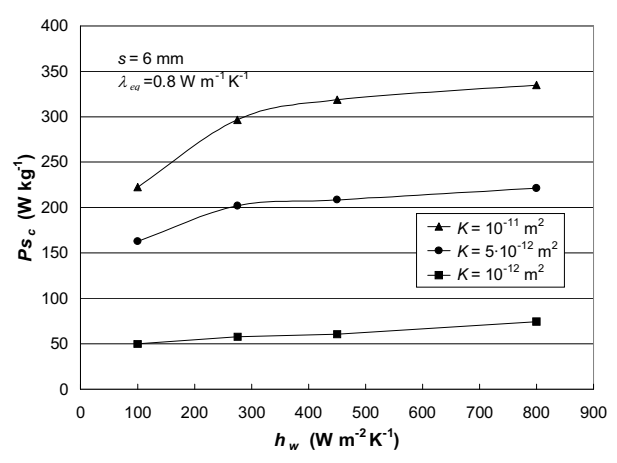


Figure 6. Influence of the wall heat transfer coefficient on calculated specific power, for s^+ and λ_{eq}^+ (see Tab. 3).

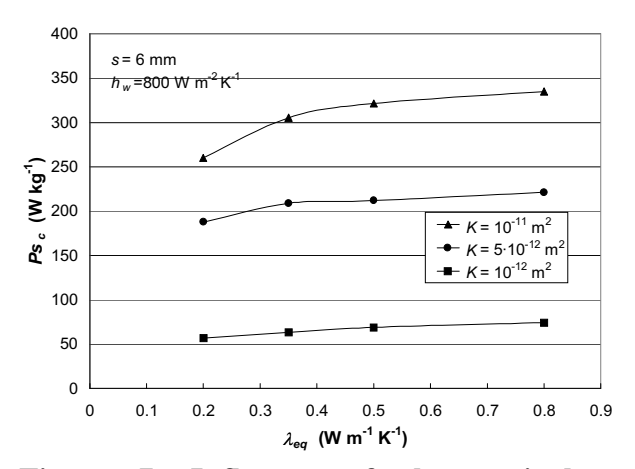


Figure 7. Influence of the equivalent thermal conductivity on calculated specific power, for s^+ and h_w^+ (see Tab. 3).

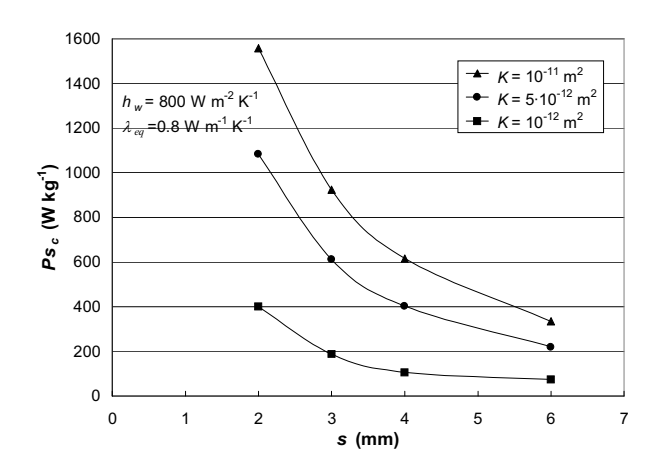


Figure 8. Influence of the adsorbent bed thickness on calculated specific power, for h_w^+ and λ_{eq}^+ (see Tab. 3).

In fact, the traditional grain-shaped adsorbent bed is characterised by a good vapour transfer between grains but a poor heat transfer. Vice-versa the consolidated bricks have good heat transfer but poor mass transfer properties. Our opinion is that the best solution should be a compromise between the relevance of the two (heat and mass) transfer phenomena. Therefore, the design of a new adsorbent bed should foresee an increase of the global heat transfer coefficient but it should be avoided that the mass transfer could becomes the new limiting factor. With this aim, it is necessary to realise thin layer of adsorbent materials or to increase the macro-porosity by using burning-out additives.

4. CONCLUSIONS

In this paper, a new technique for the preparation of tubes of a heat exchanger coated with a thin layer of zeolite was presented. This new concept allows to realise an adsorption machine with good heat and mass transfer properties. To demonstrate these features, a mathematical model for the study of the heat and mass transfer in dynamic conditions was realised. The results of the simulations of different types of adsorbent bed, show that the new bed here proposed allows to obtain the highest specific power of the adsorption cooling device.

Furthermore, a full factorial design and a sensitivity analysis allowed to evaluate the influence of the main parameters that affect the heat and mass transfer.

It was demonstrated that it is possible to enhance the competitiveness of adsorption air conditioning systems by acting on the adsorbent material shaping and thus on its thermo-physical properties.

In fact, the preparation technique developed for a new adsorbent bed allowed to increase the heat transfer properties, putting also in evidence that in this case the adsorbate permeability could become a new limiting factor.

ACKNOWLEDGEMENTS

The work here presented was supported by the CNR Progetto Finalizzato Materiali Speciali per Tecnologie Avanzate II.

5. REFERENCES

- [1]Cacciola G., Restuccia G., *Progress on adsorption heat pumps*, Heat Recovery Systems & CHP **14**, 409-420 (1994).
- [2] Cacciola G., Cammarata G., Marletta L., Restuccia G., *Macchine ad adsorbimento a ciclo rigenerativo*, La Termotecnica **47** (4), 81-90 (1993).
- [3] Alefeld G., Maier-Laxhuber P., Rothmeyer M., Zeolite heat pump and zeolite heat transformer for load management, Proceedings of the 16th Intersociety Energy Conversion Engineering Conference, Vol. 1, 855-860. Atlanta, Georgia (1981).
- [4] Restuccia G., Recupero V., Cacciola G., Rothmeyer, *Zeolite heat pump for domestic heating*, Energy **13**, 333-342 (1988).
- [5] Guilleminot J. J., Choisier A., Chaflen J. B., Nicolas S., Reymoney J. L., *Heat transfer intensification in fixed bed adsorbers*, Heat Recovery Systems & CHP **13**, 297-300 (1993).
- [6] Pons M., Laurent D., Meunier F., Experimental temperature fronts for adsorptive heat pump applications, Applied Thermal Engineering 16, 395-404 (1996).
- [7] Lang R., Westerfeld T., Gerlich A., Knoche K. F., Enhancement of heat and mass transfer in compact zeolite layers, Adsorption 2, 121-132 (1996).
- [8] Pino L., Aristov Yu., Cacciola G., Restuccia G., Composite materials based on zeolite 4A for adsorption heat pumps, Adsorption 3, 33-40 (1996).
- [9] Cacciola G., Maggio G., Restuccia G., Misura della capacità termina di adsorbenti e calcolo delle prestazioni di pompe di calore ad adsorbimento, La Termotecnica 52 (3), 67-72 (1998).
- [10] Bird R. B., Stewart W. E., Lightfoot E. N. in *Transport phenomena*, J. Wiley & Sons, New York (1960)
- [11] Ben Amar N., Sun L. M., Meunier F., *Numerical analysis of adsorptive temperature wave regenerative heat pump*, Applied Thermal Engineering **16**, 405-418 (1996).
- [12] Ferziger J. H. in *Numerical Methods for Engineering Application*, J. Wiley & Sons, London (1981).
- [13] Guilleminot J. J., Chaflen J. B., Choisie A., *Heat and mass transfer characteristics of composites for adsorption heat pumps*, Proceedings of the International

- Absorption Heat Pump Conference, AES-Vol. 31, pp. 401-406. New Orleans, Louisiana (1994).
- [14] Cacciola G., *Innovative adsorbent materials to be used in heat pump systems*, IUPAC Chemrawn IX Proceedings, pp. 131 137. Seoul, Korea, 1996.
- [15] Box G. E. P., Hunter W. G., Hunter J. S. in *Statistics for experimenters*, Wiley, New York (1978).
- [16] Johnson N. L., Leone F. C. in *Statistics and experimental design in engineering and the physical sciences*, Vol. 2, Wiley, New York (1964).

6. NOMENCLATURE

- A contact area (m²) c_p specific heat (J kg⁻¹ K⁻¹) COP coefficient of performance
- h convective heat transfer coefficient (W m⁻² K⁻¹)
- K adsorbent permeability to vapour (m²)
- L axial length of the adsorber (m)
- m mass (kg)
- p pressure (Pa)
- Ps specific power (W kg⁻¹)
- Q heat (J)
- r radial co-ordinate (m)
- R universal gas constant (J kg⁻¹ K⁻¹)
- R_e adsorber external radius (m)
- R_i adsorber internal radius (m)
- s adsorbent coating thickness $(R_e R_i)$ (m)
- t time (s)
- T temperature (K)
- v_0 vapour diffusive velocity (m s⁻¹)
- V volume (m³)
- w uptake or amount of adsorbed vapour per unit mass of anhydrous zeolite (kg kg⁻¹)

Greek symbols

- ΔH adsorption enthalpy (J kg⁻¹)
- ε_t total porosity of the solid adsorbent
- λ_{eq} equivalent thermal conductivity (W m⁻¹ K⁻¹)
- ρ density (kg m⁻³)

Subscripts

- 0 initial state
- c cooling
- con condenser
- eq equivalent
- ev evaporator
- f fluid
- *h* heating
- m metal tube
- s solid adsorbent
- v vapour phase
- w metal/adsorbent wall

Table 1. Model input data

Parameter	Symbol	Value
Initial temperature	T_0	50 °C
Initial adsorber pressure	p_0	763 Pa
Cycle maximum temperature	T_{max}	200 °C
Cycle minimum temperature	T_{min}	50 °C
Evaporator temperature	T_{ev}	3 °C
Condenser temperature	T_{con}	50 °C
Oil temperature during heating	$T_{oil.h}$	210 °C
Oil temperature during cooling	$T_{oil.c}$	40 °C
Metal tube internal radius	R_f	6 mm
Metal tube external radius	$R_{i}^{'}$	7 mm
Adsorber axial length	L	500 mm

Table 2. Typical parameters for different adsorbent configurations

Adsorbent configuration	$\frac{h_w}{\text{W m}^{-2} \text{ K}^{-1}}$	K m ²	s mm	$\mathbf{W} \overset{\lambda_{eq}}{\mathbf{m}^{-1}} \mathbf{K}^{-1}$	ρ kg m ⁻³
Grains	20	10 ⁻⁹	10	0.09	700
Brick	120	10^{-12}	5	0.42	1100
Powder	45	10^{-11}	5	0.20	800
Coating layer	800	$5 \cdot 10^{-12}$	3	0.30	800

Table 3. The 2⁴ full factorial design

Design matrix			$ \begin{array}{c} h_w \\ \text{W m}^{-2} \text{ K}^{-1} \end{array} $	K m ²	s mm	$\frac{\lambda_{eq}}{\text{W m}^{-1} \text{ K}^{-1}}$	Specific power W kg ⁻¹	
_	_	_	_	100	10^{-13}	2	0.2	26.69
+	_	_	_	800	10^{-13}	2	0.2	29.41
_	+	_	_	100	10^{-11}	2	0.2	789.19
+	+	_	_	800	10^{-11}	2	0.2	1335.67
_	_	+	_	100	10^{-13}	6	0.2	14.91
+	_	+	_	800	10^{-13}	6	0.2	18.90
_	+	+	_	100	10^{-11}	6	0.2	170.43
+	+	+	_	800	10^{-11}	6	0.2	260.00
_	_	_	+	100	10^{-13}	2	0.8	27.37
+	_	_	+	800	10^{-13}	2	0.8	30.07
_	+	_	+	100	10^{-11}	2	0.8	882.30
+	+	_	+	800	10^{-11}	2	0.8	1556.96
_	_	+	+	100	10^{-13}	6	0.8	17.65
+	_	+	+	800	10^{-13}	6	0.8	23.55
_	+	+	+	100	10^{-11}	6	0.8	222.43
+	+	+	+	800	10^{-11}	6	0.8	334.77

 Wall heat transfer coefficient:
 $h_w^- = 100 \text{ W m}^{-2} \text{ K}^{-1}$ $h_w^+ = 800 \text{ W m}^{-2} \text{ K}^{-1}$

 Vapour permeability:
 $K^- = 10^{-13} \text{ m}^2$ $K^+ = 10^{-11} \text{ m}^2$

 Adsorbent thickness:
 $s^- = 2 \text{ mm}$ $s^+ = 6 \text{ mm}$

 Thermal conductivity:
 $\lambda_{eq}^- = 0.2 \text{ W m}^{-1} \text{ K}^{-1}$ $\lambda_{eq}^+ = 0.8 \text{ W m}^{-1} \text{ K}^{-1}$

Table 4. Yates's analysis of the data

Case number	Specific power W kg ⁻¹	I	II	III	IV	Mean effect IV/8	Identity of effects
1	26.69	56.1	2180.96	2645.2	5740.3	717.54	
2	29.41	2124.86	464.24	3095.1	1438.36	179.80	h_w
3	789.19	33.81	2496.7	642.76	5363.2	670.40	\ddot{K}
4	1335.67	430.43	598.4	795.6	1407.74	175.97	$h_w K$
5	14.91	57.44	549.2	2465.38	-3615.02	-451.88	S
6	18.90	2439.26	93.56	2897.82	-1014.76	-126.85	$h_w s$
7	170.43	41.2	677.36	629.34	-3537.96	-442.25	Ks
8	260.00	557.2	118.24	778.4	-1023.7	-127.96	$h_w K s$
9	27.37	2.72	2068.76	-1716.72	449.9	56.24	λ_{eq}
10	30.07	546.48	396.62	-1898.3	152.84	19.11	$h_w \lambda_{eq}$
11	882.30	3.99	2381.82	-455.64	432.44	54.06	$K \lambda_{eq}$
12	1556.96	89.57	516	-559.12	149.06	18.63	$h_w K \stackrel{1}{\lambda}_{eq}$
13	17.65	2.7	543.76	-1672.14	-181.58	-22.70	$s \lambda_{eq}$
14	23.55	674.66	85.58	-1865.82	-103.48	-12.94	$h_w s \lambda_{eq}$
15	222.43	5.9	671.96	-458.18	-193.68	-24.21	$K s \lambda_{eq}$
16	334.77	112.34	106.44	-565.52	-107.34	-13.42	$h_w K s \lambda_{eq}$